

MODELING OF BEAM LOSSES AT ESRF

R. Versteegen*, P. Berkvens, N. Carmignani, J. Chavanne, L. Farvacque, S.M. Liuzzo, B. Nash, T. Perron, P. Raimondi, K.B. Scheidt, S. White, ESRF, Grenoble, France

Abstract

As the ESRF enters the second phase of its upgrade towards ultra low emittance, the knowledge of the beam loss pattern around the storage ring is needed for radiation safety calculations and for the new machine design optimisation. A model has been developed to simulate the Touschek scattering and the scattering of electrons on residual gas nuclei in view of producing a detailed loss map of the machine. Results of simulation for the ESRF are presented and compared with real beam measurements.

INTRODUCTION

Mapping of the electron beam losses in synchrotron light sources is needed as the beam parameters are pushed and the beam lifetime is reduced to optimise the machine performance for the users. It is necessary to anticipate the protection of various machine equipment and insertion devices from radiation damage. It is also requested from the radiation safety point of view to ensure easy access to the accelerator for maintenance. The tool developed to produce such a detailed description of beam losses, providing the electron loss locations as well as their transverse coordinates and energy when they reach the vacuum chamber aperture, is described in the first part of this paper. Simulations are then compared with experimental data taken on the ESRF storage ring. Finally, the experimental proof of principle of the foreseen collimation scheme for the machine upgrade is presented.

LOSSES FROM RANDOM PROCESSES

Three random interactions are simulated independently: elastic scattering within the bunches (Touschek losses), elastic and inelastic scattering between electrons and residual gas nuclei (Coulomb scattering and Bremsstrahlung).

Touschek losses

The Touschek effect is a large angle Coulomb scattering between two electrons inside a bunch. The transverse momentum is transferred to the longitudinal plane, which leads to the loss of one or both particles because of the limited energy acceptance of the machine [1].

The random particle generation has been developed in Matlab [2], within the Accelerator Toolbox (AT) [3]. In order to save computing resources, the lattice momentum acceptance $\Delta E/E$ is computed beforehand at each longitudinal step ds . Only particles out of the acceptance are generated and tracked to their loss point. Consequently all six coordinates are stored when the particles reach the aperture. The number of particles $N_{p,lost}$ to be generated over the full

bunch population N_{tot} is calculated using the theoretical loss rate $1/\tau_T$ as implemented in AT (Piwinski formula [4]):

$$N_{p,lost}(s) = \frac{N_{tot} ds}{c} \frac{1}{\tau_T(s)} \quad (1)$$

The initial coordinates of the particles to track $[x \ x' \ y \ y' \ z \ \delta]_{1,2}$ are randomly generated using the 6D beam matrix depending on the position along the lattice and imposing $x_1 = x_2$, $y_1 = y_2$, $z_1 = z_2$. They are selected if the energy deviation resulting from the scattering process exceeds the momentum acceptance. The scattering angle χ and hence the longitudinal momentum kick $\pm\Delta\delta = \pm\gamma v/2 |\cos \chi|$ for a colliding pair of electrons are computed according to the Møller differential cross section:

$$\frac{d\sigma}{du} = \frac{8\pi r_0^2}{(v/c)^4} \frac{u^2 - 2}{u^3} \quad (2)$$

with $u = \cos \chi$, $v = x'_1 - x'_2$ is the relative velocity of the scattering electron pair (neglecting vertical contribution), and r_0 is the classical electron radius.

The random particle generation is repeated until $N_{p,lost}(s)$ is reached. The loss locations are recorded independently from the scattering points to get the full ring loss map.

Vacuum losses

Following the same philosophy as for Touschek losses, collisions of electrons and the residual gas nuclei are simulated randomly in order to accumulate the corresponding contribution to the beam lifetime [5]. Special care was taken to be able to define a varying pressure along the lattice, and to be able to modify the gas composition and pressure locally.

Bremsstrahlung The Bremsstrahlung process is described by the Beithe-Heitler differential cross section:

$$\frac{d\sigma}{d|\delta|} = \frac{4r_0^2 Z^2}{137} \frac{1}{|\delta|} F(|\delta|) \quad (3)$$

with $F(\delta) = \left(\frac{4}{3} (1 - |\delta|) + \delta^2\right) \ln \frac{183}{Z}$, Z being the atomic number of the scattering nucleus.

The negative side of the momentum acceptance δ_m is used to compute the number of particles to track by integrating the loss probability for $|\delta| > |\delta_m|$, summing over the gas composition (α_{ij} is the number of nucleus j per molecule i constituting the gas and p_i its partial pressure):

$$\frac{N_{p,lost}}{N_{tot}} = \frac{4r_0^2 ds}{137} \left(\frac{4}{3} \ln \frac{1}{|\delta_m|} - \frac{5}{6} \right) \sum_j Z_j^2 \ln \frac{183}{Z_j^{1/3}} \sum_i \alpha_{ij} \frac{p_i}{kT} \quad (4)$$

* reine.versteegen@esrf.fr

Particles are generated within a 6D Gaussian beam distribution, and the energy loss obtained randomly according to Eq. 3 is subtracted from the sixth coordinate for the tracking.

Coulomb Scattering The Rutherford formula for small angles approximation gives the differential cross section:

$$\frac{d\sigma}{d\theta} = 8\pi \left(\frac{r_0 Z}{\gamma \beta^2} \right)^2 \frac{1}{\theta^3} \quad (5)$$

Here we need the angular acceptance of the lattice $\theta_m(s)$. The probability of interaction is obtained by integrating Eq. 5. Given the geometry of the vacuum chamber, the horizontal acceptance is much larger than the vertical and we neglect its contribution. In addition the vertical acceptance being large compared to the beam size and divergence, the particles' initial coordinates are neglected for the tracking.

ESRF loss map

The various processes contributing to the beam losses have been computed for the ESRF for the uniform filling parameters [6], using a simplified aperture model. The resulting histogram of losses from one dipole of the double bend achromat to the next is shown Fig. 1. The black elements figure the 32 lattice cells separated by the straight sections. The smallest vertical aperture is found in the in-vacuum undulators and corresponds to the highest loss peaks. The lifetime resulting from all three contributions is ~ 57 h, which is consistent with what is observed in operation. The vacuum lifetime contribution is about 30% in this mode of operation.

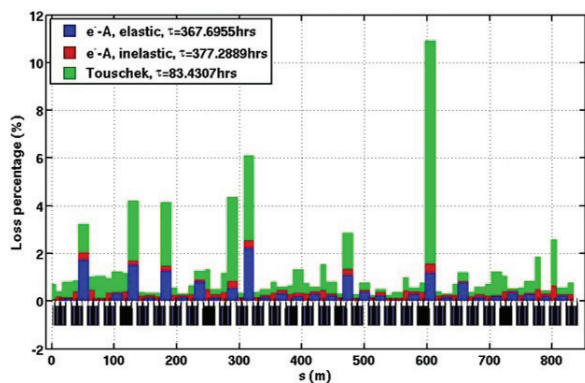


Figure 1: Simulated loss pattern for simplified aperture model at ESRF. Total lifetime is ~ 57 h.

In order to compare the simulation method to experimental data, we chose a mode allowing to distinguish the various effects and to focus on the dominant, i.e. the Touschek scattering.

TOUSCHEK LOSSES AT ESRF

A special care was taken to implement a detailed description of the aperture model for each straight section. The measurements were performed in the so called 16-bunch mode, with ~ 4 mA/bunch, to minimise the Touschek lifetime [6].

Using the scrapers (in both horizontal and vertical planes), and the Insertion Devices' (IDs) gaps height we could monitor the loss pattern evolution on the Beam Loss Detectors (BLDs). These are regularly placed on each dipole of each cell (64 detectors). The absolute calibration is not available but thanks to the periodicity of this set up, signals can be compared from one cell to another. All non in-vacuum IDs gaps were open and the vertical emittance was increased from 4 to 10 pm.rad with white noise to be insensitive to coupling fluctuation while moving the in-vacuum IDs gaps to vary the physical aperture limitations.

Beam lifetime

As a global test of the model, a first verification consisted in measuring the lifetime varying the aperture restrictions using both horizontal and vertical scrapers. Good agreement between the measurements and simulation was observed. Fig. 2 shows the case of a vertical jaw position scan.

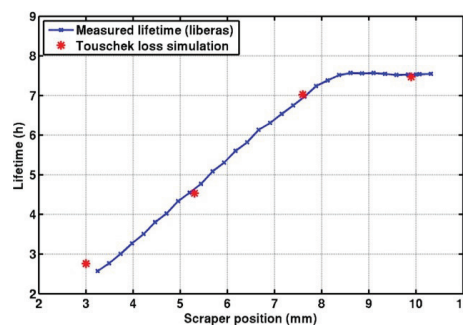


Figure 2: Beam lifetime versus vertical scraper position.

Influence of the physical aperture

Using the IDs' gaps as aperture knobs allowed to test the sensibility of the loss pattern to the local changes of physical aperture and observe the loss transfers from one location in the ring to another. It was seen that not all gaps have the same influence on the loss pattern. Loss signals resulting from the gaps' closure can be detected within less than 0.5 mm to up to 1.5 mm depending on the undulators.

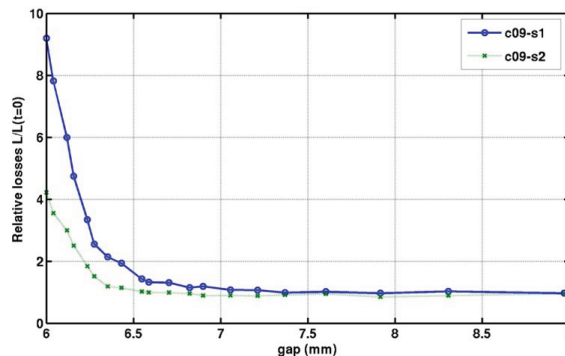


Figure 3: Loss signals downstream from ID9 (s1 and s2 refer to the first and second dipole of the cell).

The loss signals of the two detectors in cell 9 ('s1' and 's2', downstream from the in-vacuum ID) are shown in Fig. 3

Content from this work may be used under the terms of the CC BY 3.0 licence (© 2015). Any distribution of this work must maintain attribution to the author(s), title of the work, publisher, and DOI.

while closing the gap symmetrically down to ± 3 mm. It is very much compatible with the loss simulation as we obtain particle impacts concentrated within ~ 0.3 mm on each side of the vertical aperture in that same section for 6 mm gap (Fig. 4). This is a concern for loss modeling as the precision on some of the gaps' height can be as high as 0.5 mm (cells 9, 11, and 22). Consequently all the potential losses in a straight section can be concentrated within the tolerance on the gap setting, which can either double the signal or make it vanish in extreme cases.

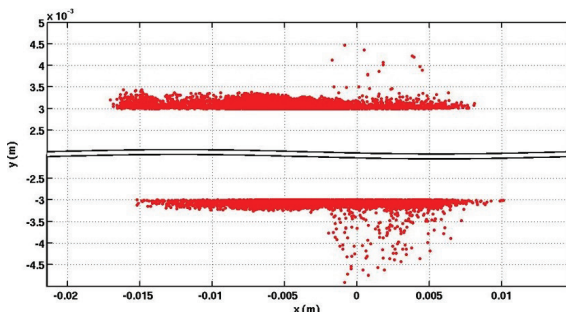


Figure 4: Simulated loss impacts on ID9 vertical aperture.

Indeed the simulation predicts high loss peaks in cells 9 and 22, which could be significantly reduced by opening slightly the gap from ± 3 mm to ± 3.2 mm. With that modification to the physical aperture model, the loss pattern around the machine is quite consistent with BLDs' signals (Fig. 5). The main expected peaks are detected in cell 2, cells 14-15-16 and in cell 27. The amplitude of the BLDs signal depends on the distance to the loss location and the resulting particle shower propagating towards the loss detector. The dose predicted by the simulation in cell 4 is not observed as it corresponds to the particles hitting the septum blade, which are shielded locally by a lead wall in the tunnel.

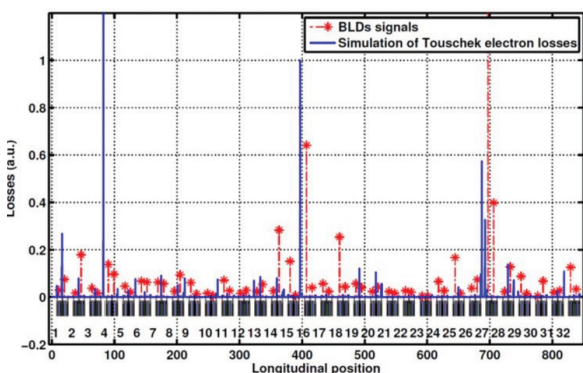


Figure 5: Comparison of BLDs' signals and Touschek loss simulation.

LOSS COLLIMATION

Protecting the IDs from radiation damage is a crucial point for the machine upgrade. It is foreseen to concentrate the losses in two or three properly shielded locations

thanks to horizontal scraper jaws, taking advantage of a high dispersion region [7]. To test the principle of such loss relocation on the operated ESRF, we used the only horizontal scraper available (with two symmetrical jaws), positioned after the injection septum where the dispersion function is not maximum.

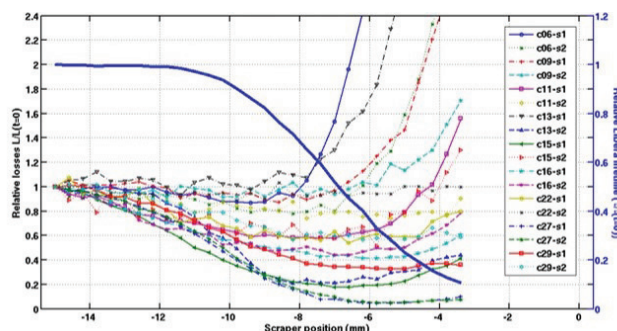


Figure 6: Loss signals versus horizontal jaw position.

The BLDs' signals located in the cells downstream of the in-vacuum undulators are reported as a function of the internal jaw position in Fig. 6. The measured beam lifetime is plotted in thick blue. As expected, the horizontal aperture restriction has a wider tuning range compared to the vertical one. The lifetime is reduced by 5 % within ~ 2 mm aperture variation (-12 to -10 mm), while with a vertical scraper the same reduction would be achieved within only 0.6 mm. When the horizontal scraper is set at about -11 mm the loss detector signals downstream of the in-vacuum IDs substantially decrease: the particles that would have been intercepted by the vertical apertures of the IDs are now stopped by the horizontal scraper. Losses increase again when closing further the scraper (to ~ -7 mm). This is due to the particle shower leakage downstream from the scraper location.

CONCLUSION

A new tool has been developed to produce a longitudinal map, element by element, of the losses around the ESRF storage ring. The model includes losses from Touschek scattering and interaction with residual gas nuclei. Comparison with experimental data showed that the model prediction are consistent with observation. The loss pattern is very dependent on the physical aperture, and can be strongly modified by opening slightly an undulator gap within its tolerance. Relocating the beam losses using horizontal scrapers with a limited impact on the lifetime proved to be feasible, which is very important for insertion devices' protection in the machine upgrade.

ACKNOWLEDGMENTS

The authors would like to thank M. Boscolo and A. Franchi for useful discussion on the beam loss modeling, B. Ogier for providing the very detailed aperture profile of all the ESRF straight sections, and H. Pedrosa Marques for discussion and input data for vacuum losses simulation.

REFERENCES

- [1] J. Le Duff, “Single and Multiple Touschek Effects”, LAL-RT-88-08 (1988).
- [2] The MathWorks, Inc., MATLAB, Natick, Massachusetts, United States.
- [3] B. Nash et al., “New functionality for beam dynamics in Accelerator Toolbox (AT)”, *These Proceedings*, MOPWA014, IPAC’15, Richmond, United States (2015).
- [4] A. Piwinski, “The Touschek Effect in Strong Focusing Storage Rings”, arXiv:physics/9903034.
- [5] A. Wrulich, “Single-beam lifetime”, CAS, CERN-94-01, p. 409 (1994).
- [6] ESRF website: <http://www.esrf.eu/Accelerators/Performance>.
- [7] R. Versteegen et al., “Collimation scheme for the ESRF Upgrade”, *These Proceedings*, TUPWA017, IPAC’15, Richmond, United States (2015).